UNIVERSITY OF
BATH

University of Bath

Synthesis of heterobimetallic tungsten acetylacetonate / alkoxide complexes and their application as molecular precursors to metal tungstates

Hamid Choujaa, Andrew L. Johnson, Gabriele Kociok-Köhn and Kieran C. Molloy[∗]

Department of Chemistry, University of Bath, Claverton Down, Bath, BA2 7AY, UK

Abstract

A series of $M_2W_2(O)_2(acac)_2(OMe)_{10}$ [M = Co (**1**), Ni(**2**), Mg (**3**), Zn (**4**)] have been synthesised and structurally characterised by X-ray crystallography. All the compounds share common structural features which are identical to the analogous molybdenum species, with four edge-sharing octahedra situated in the same plane, and incorporating two μ_3-bridging and four μ_2-bridging methoxide groups. The divalent metal M and tungsten have both octahedral coordination environments with six oxygen atoms. The structure of $Na[Zn(acac)_3]$ (**6**), a by-product of a failed synthesis of **4**, is also reported, and is a linear polymer in which $[Zn(acac)_3]^-$ anions use all six oxygen atoms to link sodium cations either side of the anion.

Thermal decomposition of representative samples (**1**, **3**) shows them to be single-source precursors for metal tungstates MWO_4. When the decomposition is carried out under an autogenerated pressure (RAPET) at 700 ^{o}C **1** forms $CoWO_4$ nanoparticles, along with WOx-filled carbon nanotubes and amorphous carbon, while **3** forms $MgWO_4$ nanoparticles and rods, though the latter lack a carbon shell and are much shorter in length.

Keywords: Tungsten, alkoxide, β-diketonate, mixed-metal, X-ray, thermal decomposition

---

[∗] Corresponding author, tel: +44 1225 386382
e-mail: k.c.molloy@bath.ac.uk (K C Molloy)

Introduction

Tungsten oxide thin films have a number of applications e.g. electrochromic, photochromic displays,[1] photocatalysts,[2-4] gas sensors,[5] solar control coatings,[6] particularly when in thin film format. Such films are usually produced either by hydrolysis of a suitable precursor in a sol-gel protocol,[7] or by chemical vapour deposition (CVD) from a volatile precursor.[8-10] The properties of these films can be modified by the inclusion of a variety of additional metals,[11-13] which from a technological perspective require co-hydrolysis of two metal moieties (sol-gel) or a dual-source CVD approach. One variation which removes the practical difficulties of matching hydrolysis / decomposition rates is the use of a single-source precursor (SSP) which incorporates both metals in the same molecule. In this paper we explore the synthesis of W-O-M type compounds and their thermal decomposition to mixed metal oxides.

This preparation of heterometallic, heteroleptic acetylacetonate / alkoxide complexes of type $M_aM_b(acac)_x(OR)_y$ has been widely used as a way of controlling the properties of the molecule by virtue of the distinct ligand types therein.[14] $MAl_2(acac)_4(OPr^i)_4$ (M = Co, Ni, Mg) were first synthesised by Mehrotra *et al.* by modification of mixtures of the homoleptic alkoxides with acetylacteone.[15] Since then, other related compounds such as $Co_2Zr_2(acac)_2(OPr^n)_{10}$,[16] $Mo_2M_2(O)_2(acac)_2(OMe)_{10}$ (M = Co, Ni),[17] $Co_2Ti_2(acac)_2(OPr^i)_{10}$ [18] and $Co_2Al_2(acac)_4(OPr^i)_6$ [19] have been described. In particular, the interaction of $M'(acac)_2$ (M' = Co, Ni, Zn or Mg) with $M(OMe)_5$ (M = Ta, Nb) in a hydrocarbon solvent was found to provide $M'_2M_2(acac)_2(OMe)_{12}$ and $M(acac)(OMe)_4$.[20] Of more direct relevance, mixed Mo-O-M species $Mo_2M_2(O)_2(acac)_2(OR)_{10}$ have been reported by others,[17] and herein we extend this family to cover the tungsten analogues.

Experimental Section

General Procedures: Elemental analyses were performed using an Exeter Analytical CE 440 analyser. ^1H and $^{13}C\{^1H\}$ NMR spectra were recorded on a Bruker Advance 300 MHz FT–NMR spectrometer, as saturated solutions at room temperature, unless stated otherwise; chemical shifts are in ppm with respect to Me_4Si, coupling constants are in Hz.

All manipulations were carried out under a dry nitrogen or argon atmosphere using standard Schlenk techniques and standard glove-box. All dry solvents were purified by an Innovative Technology Inc. solvent purification system (SPS). $[W(O)(OMe)_4]_2$ was synthesised according literature procedure.[21]

Commercial $Zn(acac)_2.xH_2O$ (x = 1.84; measured by TGA) was purchased from Aldrich and dried with dry toluene and subsequently evaporated; this process was repeated twice and the product sublimed twice under vacuum to provide an anhydrous Zn(acac). $Co(acac)_2$, $Ni(acac)_2$ were purchased from Aldrich and were dried by vacuum sublimation. $Mg(acac)_2$ was prepared by refluxing magnesium metal with an excess of acetylacetone. The resulting slurry was filtered and the powder obtained was washed with boiling toluene and evaporated to dryness. Co(acac)(OMe),[22] Ni(acac)(OMe),[23] Mg(acac)(OMe)[24] were synthesised according to the literature procedures.

Complexes **1** - **4** can be prepared by an adaptation of literature methodology previously used to successfully prepare analogous molybdenum compounds.[20] However, in the cases of **1** – **3** an alternative route, in which M(acac)(OMe) M = Co, Ni, Mg) was first prepared and isolated, proved to be less wasteful of reagents and is described below; only in the case of **4** was this alternative procedure unsuccessful.

Synthesis of $Co_2W_2(O)_2(acac)_2(OMe)_{10}$(1)

$WO(OMe)_4$ (2.001 g, 6.17 mmol) and Co(acac)(OMe) [22] (1.185 g, 6.14 mmol) were dissolved in dry toluene (80 mL). The reaction medium was refluxed for 30 min. The yellow solution was cooled to room temperature and then concentrated to afford purple crystals. After standing at 3°C for 12 hours, the crystals were separated by filtration and dried *in vacuo* (yield 80%, m.p. > 230 °C). Found (calc. for $C_{20}H_{44}Co_2O_{16}W_2$): C 22.7 (23.4), H 3.9 (4.3) %.

Also prepared by the same method were:

$Ni_2W_2(O)_2(acac)_2(OMe)_{10}$ (2) : Yield 85 %, m.p. >230 °C. Found (calc. for $C_{20}H_{44}Ni_2O_{16}W_2$): C 22.0 (23.4) H 4.0 (4.3) %

Mg$_2$W$_2$(O)$_2$(acac)$_2$(OMe)$_{10}$ (3) : Yield 85 %. m.p > 230°C. Found (Calc. for C$_{20}$H$_{44}$Mg$_2$O$_{16}$W$_2$): C 25.8 (25.1) H 4.7 (4.6) %. ^{1}H NMR (CDCl$_3$, 300 MHz, 298 K, δ ppm) : 1.88 (s, 12H, acac, -C**H$_3$**), 3.90 (s, 6H, μ$_3$-OC**H$_3$**), 4.39 (s, 12H, terminal-OC**H$_3$**), 4.61 (s, 12H, μ$_2$-OC**H$_3$**), 5.28 (s, 2H, acac -CH-). ^{13}C NMR (CDCl$_3$, 300 MHz, 298 K, δ ppm) : 28.3 (s, -O**C**H$_3$), 55.1 (μ$_2$-O**C**H$_3$), 63.8 (μ$_3$-O**C**H$_3$), 65.0 (μ$_3$-O**C**H$_3$), 99.6 (acac, -**C**H-), 191.0 (acac, -**C**-).

Synthesis of Zn$_2$W$_2$(O)$_2$(acac)$_2$(OMe)$_{10}$ (4): WO(OMe)$_4$ (1.3 g, 4.01 mmol) and Zn(acac)$_2$ (0.503 g, 1.91 mmol) were dissolved in dry toluene (20 mL). The reaction medium was refluxed for 15 min. and allow to cool to room temperature and then concentrated to afford purple crystals of **4**. After standing at 3°C for 12 hours, the crystals are separated by filtration and then dried *in vacuo.* Yield = 34 %, m.p .> 230°C. Found (Calc. for C$_{20}$H$_{44}$O$_{16}$W$_2$Zn$_2$): C 22.5 (23.1) H 4.0 (4.3) %. ^{1}H NMR (CDCl$_3$, 300 MHz, 298 K, δ ppm) : 1.91 (s, 12H, acac, -C**H$_3$**), 3.98 (s, 6H, μ$_3$-OC**H$_3$**), 4.52 (s, 24H, terminal and μ$_2$-OC**H$_3$**), 5.26 (s, 2H, acac, -C**H**-) ^{13}C NMR (CDCl$_3$, 300 MHz, 298 K, δ ppm): 28.2 (terminal -O**C**H$_3$), 56.9 (μ$_2$-O**C**H$_3$), 64.6 (μ$_3$-O**C**H$_3$), 98.9 (s, 1H, acac, -**C**H-), 191.8 (s, acac, -**C**-).

The mother liquor was concentrated to give, after standing at -20°C for 12 hours, the by-product WO(OMe)$_3$(acac) **(5)**. Mp = 56°C, ^{1}H NMR (C$_7$D$_8$, 300 MHz, 298 K, δ ppm): 1.70 (s, 3H, acac, -C**H$_3$**), 1.75 (s, 3H, acac, -C**H$_3$**), 4.41 (s, 6H, -OC**H$_3$**), 4.65 (s, 3H, -OC**H$_3$**-), 5.16 (s, 1H, acac, -C**H**-).^{13}C NMR (C$_7$D$_8$, 300 MHz, 298 K, δ ppm) : 27.2 (acac, -**C**H$_3$), 63.3 (O**C**H$_3$), 65.3 (O**C**H$_3$), 104.2 (acac, -**C**H-), 186.4 (s, acac **C**), 194.2 (acac, -**C**-).

Thermodecomposition under "Reaction under autogenic pressure at elevated temperatures" (RAPET)

The thermal decomposition under RAPET conditions of Co$_2$W$_2$O$_2$(acac)$_2$(OMe)$_{10}$ (**1**) and Mg$_2$W$_2$O$_2$(acac)$_2$(OMe)$_{10}$ (**3**) were carried out in a 5 mL closed vessel cell. The cell was assembled from stainless steel Swagelok parts. A ½ inch union part was capped on both sides by standard plugs. For these syntheses, 0.5 g of **1** and **3** were introduced into the vessel at room temperature in a nitrogen atmosphere of the glove-box. The filled cell was closed tightly with the other plug and then placed inside an iron pipe in the middle of the furnace. The temperature was raised at a rate of 10°C per minute. The

closed vessel reactor (Swagelok) was heated at 700°C for 2 h, then, gradually cooled (1°C / min.) to room temperature, opened with the release of a little pressure, and the residual dark black powder collected. The total recovered mass of the above RAPET reactions are respectively 62% and 59%. All yields are relative to the weight of the starting materials.
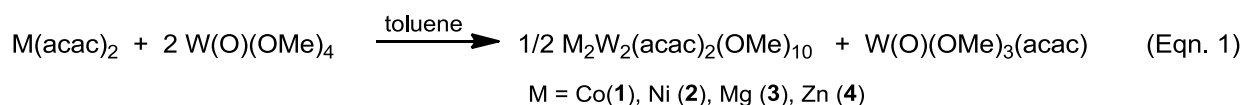
Thermal decomposition in air

The decomposition in the air was carried out in a graphite reactor pot containing 0.5 g of $Co_2W_2O_2(acac)_2(OMe)_{10}$ (**1**) placed in the middle of a tube furnace. The temperature was raised at a rate of 10°C per minute. The graphite vessel was heated at 700°C for 1 h and then gradually cooled (1°C / min.) to room temperature, leaving a grey-blue powder product.

Crystallography

Experimental details relating to the single-crystal X-ray crystallographic studies are summarised in Table 1. For all structures, data were collected on a Nonius Kappa CCD diffractometer at 150(2) K using Mo-K_α radiation (λ = 0.71073 Å). Structure solution followed by full-matrix least squares refinement and was performed using the WinGX-1.70 suite of programmes.[25] Corrections for absorption were made in all cases.

Results and Discussion

Following the methodology used to prepare the analogous molybdenum compounds,[20] heterobimetallic tungsten acetylacetonate alkoxides $M_2W_2(O)_2(acac)_2(OMe)_{10}$ [M = Co (**1**), Ni (**2**), Mg (**3**), Zn (**4**)] have been synthesised first by reacting two equivalents of $WO(OMe)_4$ and one equivalent of $M(acac)_2$ in refluxing toluene solvent (Eq. 1); yields were in the range 31 – 34 %.

$$M(acac)_2 \ + \ 2\ W(O)(OMe)_4 \ \xrightarrow{\text{toluene}} \ 1/2\ M_2W_2(acac)_2(OMe)_{10} \ + \ W(O)(OMe)_3(acac) \qquad \text{(Eqn. 1)}$$
$$M = Co(\mathbf{1}),\ Ni\ (\mathbf{2}),\ Mg\ (\mathbf{3}),\ Zn\ (\mathbf{4})$$

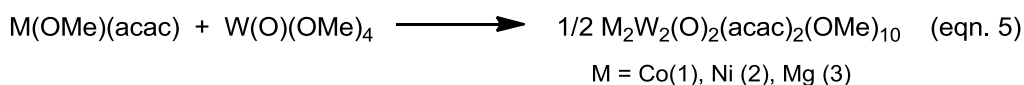However, this approach requires the use of second equivalent of $W(O)(OMe)_4$ which is transformed into the unwanted by-product $W(O)(OMe)_3(acac)$ by the following series of reactions:

$$M(acac)_2 \; + \; W(O)(OMe)_4 \longrightarrow M(OMe)(acac) \; + \; W(O)(OMe)_3(acac) \qquad \text{Eqn. 2}$$

$$M(OMe)(acac) \; + W(O)(OMe)_4 \longrightarrow 1/2 \; M_2W_2(O)_2(acac)_2(OMe)_{10} \qquad \text{Eqn 3}$$

In order to removed the need to separate $W(O)(OMe)_3(acac)$ from the final reaction mixture, and to avoid waste of the starting tunsten oxo-alkoxide, we have prepared **1 – 3** by an alternative strategy in which the intermediate M(OMe)(acac) is first synthesised independently:[22]

$$M(acac)_2 \; + \; M'OH \xrightarrow[\text{M' = K, Na}]{\text{MeOH}} 1/4 \; [M(acac)(OMe)(HOMe)]_4 \xrightarrow[ca.\ 100^\circ C]{\text{heat}} M(acac)(OMe) \qquad \text{Eqn. 4}$$
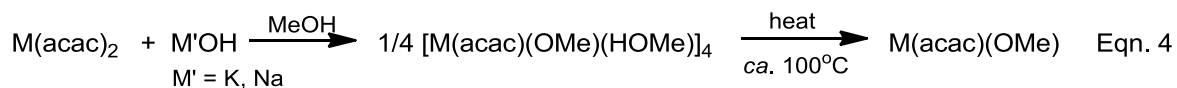
MeOH is removed by heating M(OMe)(acac)(HOMe) to $ca.100\ ^\circ C$ before further reaction,[23] as the corresponding molydenum compounds have been found to be susceptible to decomposition *via* methanolysis.[20] A stoichiometric reaction of M(acac)(OMe) with $W(O)(OMe)_4$ then affords the desired products in *ca.* 80% yield.

$$M(OMe)(acac) \; + \; W(O)(OMe)_4 \longrightarrow 1/2 \; M_2W_2(O)_2(acac)_2(OMe)_{10} \qquad \text{(eqn. 5)}$$
$$M = Co(1),\ Ni\ (2),\ Mg\ (3)$$

Only in the case of M = Zn (**4**) did this approach fail, with $NaZn(acac)_3$ (**6**) being the only product isolated; **4** was thus prepared by the route of eqn. 1, and $W(O)(OMe)_3(acac)$ (**5**) isolated and confirmed as the reaction by-product. As far as we are aware, **5** has not been reported previously.

All of these compounds $M_2W_2(O)_2(acac)_2(OMe)_{10}$ **1 - 4** are isostructural in terms of symmetry and space group and differ only in the nature of M. Despite the difference in the size of the divalent metal M^{II}, all the triclinic structures are quasi-identical in regard with the bond lengths and angles (Table 2); M-O bond lengths in **1 -4** are comparable to the ranges of distances observed in the structure

$M_2M'_2O_2(acac)_2(OMe)_{10}$ (M = Co, Ni, Mg, Zn) and M' = Ta and Nb.[20]. The discussion herein is restricted to the M = Co (**1**) as typical.

The structure of **1** incorporates centrosymmetric $Co_2W_2O_2(acac)_2(OMe)_{10}$ molecules (Fig.1; Table 1). **.** And follows the well-known $[Ti(OMe)_4]_4$ structural type:[26] four edge-sharing octahedra situated in the same plane, two μ_3-triply bridging and four μ_2-doubly bridging methoxide groups. The metal divalent M and tungsten have both octahedral coordination environments with six oxygen atoms. The octahedra surrounding the cobalt and tungsten atom are distorted because of the different types of oxygen atoms (terminal-OMe, bridging μ_2-OMe and μ_3-OMe). The *trans* O-W-O angles vary between 162.87(16) $^{\circ}$ and 165.68(16) $^{\circ}$ and are small compared to the ideal angle of 180°. Moreover, the longest bond W-O(4) [2.170(3) Å] is in the position *trans* to the shortest bond which is the double bond W=O(6) [1.710(3) Å]. Also, the terminal methoxy ligands O(7) and O(8) are respectively *trans* to the bridging μ_2-O(5) and μ_2-O(3). The shortest Co-O distances in 1 involve the two oxygen atoms of the acac ring. The observed Co–O and W-O distances are in agreement respectively with those found in $[Co(acac)(OMe)(MeOH)]_4$ [22] and $WO(OMe)_4$.[21] Moreover, the heterobimetallic compounds obtained with tungsten are consistent with their analogues incorporating molybdenum *e.g* $Co_2Mo_2(O)_2(acac)_2(OMe)_{10}$.[17]

The three different OMe environments are clearly visible in the ^{1}H and ^{13}C NMR spectra of diamagnetic **3**, corresponding to terminal (4.61, 55.1 ppm for ^{1}H, ^{13}C, respectively, integration = 12H), μ_2-OMe (4.39, 63.8 ppm, integration = 12H) and μ_3-OMe (3.90, 55.1 ppm, integration = 6H) environments, implying retention of the solid-state structure in solution. In the case of **4**, similar ^{1}H NMR spectra are, however, only seen at 233 K; thus, while a sharp signal for the μ_3-OMe (3.98 ppm, integration = 6H) is visible at 303 K, at this temperature signals for the μ_2-OMe and terminal OMe coalesce into a broad, 24H signal at 4.52 ppm. On cooling to 233 K, this broad signal splits into two (4.46, 4.58 ppm), which implies a more facile exchange between these two OMe environments in the case of the zinc compound. The related compound $Mg_2Ta_2(acac)_2(OMe)_{12}$ displays similar behavior of intermolecular exchange but seems to involve a different pair of methoxy groups *i.e* bridging μ_2- and μ_3-OMe; molecular rigidity at ambient temperature has, however, been noted for $Zn_2Ta_2(acac)_2(OMe)_{12}$.[20]

We also now report the structure of $Na[Zn(acac)_3]$ (**6**), formed unintentionally in the zinc variation of Eqn. 5. **6** is a known compound which has been the subject of infrared analysis but not structurally

characterized.[27, 28]. **6** adopts a linear polymeric structure in which both metals alternate along a three-fold axis (Fig. 2). The three acac groups coordinate in a *tris-chelate* manner to form a six-coordinate $[Zn(acac)_3]^-$ anion. In addition, each of the six oxygen atoms of the three acac ligands bridges to an adjacent sodium, three on each side of the anion, making the sodium also six-coordinate; the Zn…Na separation is 2.9614 Å. The only directly comparable structure is that of Na[Zn(3-CNacac)_3].EtOH, in which the zincate anion is analogous to that in **6**, but the cations are linked through three oxygens of acac groups and two nitrogen atoms of the 3-CN functionality of the β-diketonate; the N_2O_4 coordination at sodium is completed by coordination of the ethanol solvate. Unlike **6**, the increased functionality of the 2-CNacac ligand leads to a three-dimensional structure and a longer Zn…Na separation [3.195(2) Å].[29]

TGA data for **1** - **4** are shown in Fig. 3. All four compounds decompose in a broadly concerted manner with no clear separation of the individual processes, save for the final stage in the decomposition of **3** at T > 500 ^{o}C. In the case of **2**, there is a small weight loss (5.1 %) at *ca.* 220 ^{o}C not seen in the other samples which we attribute to loss of residual solvent in this sample; the final residual mass in this case has been revised taking this into account. The residual mass for each compound is consistent with MWO_4 as the final product [found, calculated: 58.1, 59.8 (**1**); 59.8, 59.6 (**2**); 53.7, 56.9 (**3**); 60.7, 60.3 % (**4**)]. Microanalysis of the product of the thermal decomposition of **1** in air at 700°C [C: 0.06; H 0.0 %] shows that all the organic matter has been cleanly removed, and PXRD of the grey-blue product (Fig. 4) can be indexed to monoclinic $CoWO_4$ (PDF 15-0867). There is no regularity to the morphology of the decomposition product.

For comparison, we have also decomposed **1** and **3** under an autogenerated pressure in a sealed container at 700 ^{o}C, a process termed RAPET (Reaction under Autogenic Pressure at Elevated Temperatures).[30] In both cases there is considerable residual carbon in the final black product(s) [**1**: C 19.1, H 0.3; **3**: C 18.5, H 0.2 %], though this must be amorphous as the PXRD patterns again match those of MWO_4 (Fig. 5). In the case of precursor **1** PXRD again confirms the formation of monoclinic $CoWO_4$; TEM (Fig. 6a) shows the product consists of both a light element (presumably carbon, as the light contrast image) along with embedded aggregates of nanoparticles (upto *ca.* 100 nm in width) containing heavier elements ($CoWO_4$, which appear as the dark contrast image) and rods, which comprise a lighter element outer shell with a heavy element interior (Fig. 6b) as a minor component (Fig 6c); EDX of these rods,

which can grow upto *ca.* 1000nm in length (Fig. 6c) reveal only tungsten (and no cobalt), and appear to be WO_x-filled carbon nanotubes, as we have observed in the decomposition of various tungsten aminoalkoxides.[31]

In the case of the decomposition of **3** the product is tetragonal $MgWO_4$ (Fig. 5) and seems more homogeneous in nature i.e. SEM shows small and large particulates but no rods (Fig. 7a). TEM (Fig. 7b) again reveals both a light element component (presumably, again, carbon) and heavy element-containing nanoparticles, some of which grow into longer rods, albeit small in length (*ca.* 150 nm) compared to those from precursor **1**; these rods, however, do contain both Mg and W by EDX, so seem to be $MgWO_4$ with no visual suggestion of these being encased within a carbon shell.

Conclusions

The bimetallic precursors $W_2M_2(O)_2(OMe)_{10}(acac)_2$ (M = Co, Ni, Mg, Zn) have been prepared in an efficient manner from the reaction of $W(O)(OMe)_4$ and $M(OMe)(acac)$. The molecular structures of all four compounds are similar and replicate those of their molybdenum analogues. Representative examples (M = Co, Mg) show these compounds are single-source precursors for MWO_4 materials.

Supporting Information

Crystallographic data for the structural analysis (in CIF format) have been deposited with the Cambridge Crystallographic Data Centre, CCDC. Copies of this information may be obtained from the Director, CCDC, 12 Union Road, Cambridge, CB21EZ, UK (Fax: +44-1233-336033; e-mail: deposit@ccdc.cam.ac.uk.

References

[1]   P.M.S. Monk, R.J. Mortimer, M.J. Rosseinsky, Electrochromism: Fundamentals and Applications, VCH, New York, 1995.

[2]   S.H. Baeck, K.S. Choi, T.F. Jaramillo, G.D. Stucky, E.W. McFarland, Adv. Mater. 15 (2003) 1269.

[3]   S. Ikeda, T. Itani, K. Nango, M. Matsumura, Catal. Lett. 98 (2004) 229.

[4]   B. Yang, P.R.F. Barnes, Y. Zhang, V. Luca, Catal. Lett. 118 (2007) 280.

[5]   K. Zakrzewka, Thin Solid Films 391 (2001) 229.

[6]   C.G. Granqvist, Sol. Energy Mater. 91 (2007) 1529.

[7]   C.O. Avellaneda, L.O.S. Bulhoes, Solid State Ionics 165 (2003) 117.

[8]   W.B. Cross, I.P. Parkin, S.A. O'Neill, P.A. Williams, M.F. Mahon, K.C. Molloy, Chem. Mater. 15 (2003) 2786.

[9]   K.C. Molloy, P.A. Williams, Appl. Organomet. Chem. 22 (2008) 560.

[10] K.C. Molloy, P.A. Williams, Appl. Organomet. Chem. 22 (2008) 676.

[11] S. Sitkiewitz, A. Heller, New J. Chem. 20 (1996) 233.

[12] A.L. Linsebigler, G. Lu, J.T. Yates, Chem. Rev. 95 (1995) 735.

[13] A. Hameed, M.A. Gondal, Z.H. Yamani, Catalysis Commun. 5 (2004) 715.

[14] G.A. Seisenbaeva, E.V. Suslova, M. Kritikos, V G Kessler, L. Rapenne, M. Andrieux, F. Chassagneux, S. ParolaJ. Mater. Chem. 14 (2004) 3150.

[15] R.C. Mehrotra, Coord. Chem. 21 (1981) 113.

[16] G.A. Seisenbaeva, S. Gohi, V.G. Kessler, J. Mater. Chem. 14 (2004) 3177.

[17] P. Werndrup, G.A. Seisenbaeva, G. Westin, I. Persson, V.G. Kessler, Eur. J. Inorg. Chem. (2006) 1413.

[18] V.G. Kessler, S. Gohil, S. Parola, Dalton Trans. (2003) 544.

[19] E. Suslova, G.A. Seisenbaeva, V.G. Kessler, Inorg. Chem. Comm. 5 (2002) 946.

[20] P. Werndrup, V.G. Kessler, J. Chem. Soc., Dalton Trans. (2001) 574.

[21] W. Clegg, R.J. Errington, P. Kraxner, C. Redshaw, J.Chem. Soc., Dalton Trans (1992) 1431.

[22] J.A. Bertrand, A.P. Ginsberg, R.I. Kaplan, C.E. Kirkwood, R.L. Martin, R.C. Sherwood, Inorg. Chem. 10 (1971) 240.

[23]   J.A. Bertrand, D. Caine, J. Amer. Chem. Soc. 86 (1964) 2298.

[24]   M.A. Halcrow, J.-S. Sun, J.C. Huffman, G. Christou, Inorg. Chem. 34 (1995) 4167.

[25]   L.J. Farrugia, J. Appl. Crystallogr. 32 (1999) 837.

[26]   D.A. Wright, D.A. Williams, Acta Crystallogr. B24 (1968) 1107.

[27]   F.P. Dwyer, A.M. Sargeson, Journal and Proceedings of the Royal Society of New South Wales 90 (1956) 29.

[28]   M.L. Niven, G.C. Percy, Transition Met. Chem. 3 (1978) 267.

[29]   O. Angelova, J. Macicek, G. Petrov, J. Coord. Chem. 24 (1991) 305.

[30]   S.V. Pol, V.G. Pol, L. Gedanken, Chem. - Eur. J. 10 (2004) 4467

[31]   H. Choujaa, A.L. Johnson, G. Kociok-Köhn, K.C. Molloy, Dalton Trans. 41 (2012) 11393.

Table 1. Crystal data and structure refinement for **1** – **4**, **6**.

	1	2	3	4	6
Chemical formula	$C_{20}H_{44}Co_2O_{16}W_2$	$C_{20}H_{44}Ni_2O_{16}W_2$	$C_{20}H_{44}Mg_2O_{16}W_2$	$C_{20}H_{44}O_{16}W_2Zn_2$	$C_{15}H_{21}NaO_6Zn$
Formula Mass	1026.11	1025.67	956.87	1038.99	385.68
Crystal system	Triclinic	Triclinic	Triclinic	Triclinic	Trigonal
$a/Å$	8.00630(10)	8.00460(10)	8.01650(10)	8.0163(4)	16.2290(3)
$b/Å$	10.53970(10)	10.5277(2)	10.57730(10)	10.5610(6)	16.2290(3)
$c/Å$	10.8346(2)	10.7933(2)	10.8150(2)	10.8366(7)	11.8456(3)
$α/°$	111.8997(5)	112.0450(10)	111.9780(10)	111.976(3)	90.00
$β/°$	91.4626(6)	91.4130(10)	91.2740(10)	91.301(3)	90.00
$γ/°$	111.6172(6)	111.6310(10)	111.7630(10)	111.685(2)	120.00
Unit cell volume/$Å^3$	774.430(19)	769.53(2)	775.858(19)	776.64(8)	2701.91(10)
Temperature/K	150(2)	150(2)	150(2)	150(2)	150(2)
Space group	$P\bar{1}$	$P\bar{1}$	$P\bar{1}$	$P\bar{1}$	$R\bar{3}c$
Z	1	1	1	1	6
No. of reflections measured	18262	14711	14803	5821	12033
No. of independent reflections	4459	4461	4524	2841	687
R_{int}	0.0988	0.1720	0.0446	0.0592	0.0405
Final R_1 values ($I > 2σ(I)$)	0.0434	0.0728	0.0243	0.0538	0.0255
Final $wR(F^2)$ values ($I > 2σ(I)$)	0.1114	0.1803	0.0588	0.1288	0.0669
Final R_1 values (all data)	0.0443	0.0747	0.0251	0.0666	0.0265
Final $wR(F^2)$ values (all data)	0.1125	0.1842	0.0593	0.1354	0.0678
Goodness of fit on F^2	1.060	1.050	1.117	1.031	1.134
CCDC number	923394	923395	923396	923397	923398

Table 2. Selected geometric data for **1** - **4**

M =	Co (**1**)	Ni (**2**)	Mg (**3**)	Zn (**4**)
W-O(3)	2.004(3)	2.008(5)	2.009(2)	1.997(7)
W-O(4)	2.170(3)	2.167(5)	2.1607(19)	2.156(7)
W-O(5)	2.005(3)	2.003(5)	2.0044(18)	1.993(7)
W-O(6)	1.710(3)	1.712(5)	1.708(2)	1.713(8)
W-O(7)	1.868(3)	1.853(6)	1.860(2)	1.843(7)
W-O(8)	1.883(3)	1.878(5)	1.878(2)	1.858(7)
M-O(1)	2.017(3)	1.992(5)	2.014(2)	2.002(7)
M-O(2)	2.015(3)	1.987(5)	2.0127(19)	2.010(7)
M-O(3)	2.118(4)	2.077(5)	2.085(2)	2.118(7)
M-O(4)	2.142(3)	2.102(4)	2.134(2)	2.145(7)
M-O(4')	2.142(3)	2.097(5)	2.1199(19)	2.144(6)
M-O(5')	2.109(3)	2.073(5)	2.093(2)	2.138(7)

Bond angles (^{o})

	Co (**1**)	Ni (**2**)	Mg (**3**)	Zn (**4**)
O(3)-W-O(4)	75.50(12)	75.19(19)	75.03(8)	74.7(3)
O(3)-W-O(5)	86.19(14)	86.4(2)	85.82(8)	86.3(3)
O(3)-W-O(6)	92.62(17)	92.1(3)	92.65(10)	92.8(3)
O(3)-W-O(7)	90.56(16)	90.9(3)	90.42(9)	90.2(3)
O(3)-W-O(8)	165.68(16)	165.9(2)	165.36(10)	165.2(3)
O(4)-W-O(5)	74.95(11)	74.56(17)	74.51(7)	74.7(2)
O(4)-W-O(6)	162.87(16)	161.9(3)	162.18(10)	161.8(3)
O(4)-W-O(7)	89.09(14)	89.4(2)	89.61(9)	89.7(3)
O(4)-W-O(8)	90.37(14)	90.8(2)	90.55(8)	90.7(3)
O(5)-W-O(6)	92.23(17)	92.1(3)	92.06(10)	91.5(3)
O(5)-W-O(7)	164.02(17)	163.9(3)	164.12(11)	164.5(3)
O(5)-W-O(8)	87.89(14)	87.8(2)	87.92(8)	87.4(3)
O(6)-W-O(7)	103.56(18)	103.9(3)	103.53(12)	103.8(4)
O(6)-W-O(8)	100.63(16)	101.0(2)	100.80(11)	100.7(4)
O(7)-W-O(8)	91.57(16)	91.1(3)	92.02(10)	92.3(3)
O(1)-M-O(2)	91.36(13)	92.58(19)	89.43(8)	91.7(3)
O(1)-M-O(3)	93.45(13)	93.7(2)	93.08(9)	93.4(3)
O(1)-M-O(4)	165.31(12)	166.53(18)	165.60(9)	163.8(3)
O(1)-M-O(4')	93.15(12)	92.70(18)	94.27(8)	93.9(3)
O(1)-M-O(5')	97.75(13)	95.58(19)	98.26(9)	98.5(3)
O(2)-M-O(3)	94.23(14)	93.6(2)	95.47(9)	95.7(3)
O(2)-M-O(4)	96.76(12)	95.68(19)	98.17(8)	97.5(3)
O(2)-M-O(4')	167.04(13)	167.9(2)	166.25(9)	164.8(3)
O(2)-M-O(5')	93.87(13)	94.0(2)	92.74(9)	93.0(3)
O(3)-M-O(4)	73.81(12)	75.19(19)	75.03(8)	72.6(3)
O(3)-M-O(4')	97.62(13)	96.9(2)	97.55(8)	98.1(3)
O(3)-M-O(5')	166.01(13)	167.7(2)	166.05(9)	165.1(3)

O(4)-M-O(4')	81.61(11)	81.29(19)	81.23(8)	80.5(3)
O(4')-M-O(5')	73.49(11)	74.69(19)	73.63(8)	72.2(2)

Symmetry transformations used to generate equivalent atoms ('): 1-x, 1-y, 2-z (**1**, **2**); 1-x, -y, 2-z (**3**); -x, -y, 2-z (**4**)

Figure Captions

Figure 1.   (a) The asymmetric unit of M = Co (**1**), Ni (**2**), Mg (**3**), Zn (**4**) showing the labelling scheme used; thermal ellipsoids are at the 50% probability level. Symmetry operation: 1-x,1-y,2-z.

Figure 2.   The asymmetric unit of **6** showing the labelling scheme used; thermal ellipsoids are at the 50% probability level. Selected geometric data :Zn-O 2.0755(10), Na-O 2.3332(10), C(1)-O 1.2686(17) Å; O-Zn-O^a 87.16(5), O-Zn-O^b 85.50(4), O-Zn-O^d 103.17(6), O-Zn-O^e 168.17(6), O-Na-O^c 74.29(4), O-Na-O^f 180.00(6), O-Na-O^g 105.71(4), O-Na-O^h 105.71(4) $^\circ$. Symmetry operations: (a) y,x,-z+1/2, (b) -x+y,-x,z, (c) -y,x-y,z, (d) x-y,-y,-z+1/2, (e) -x,-x+y,-z+1/2, (f) -x,-y,-z, (g) y,-x+y,-z, (h) x-y,x,-z

Figure 3.   TGA data for **1 – 4**

Figure 4.   PXRD of the product of the thermal decomposition of **1** in air at 700 ^{o}C; lines are indexed to monoclinic CoWO$_4$ (PDF 15-0867).

Figure 5.   PXRD of the product of the thermal decomposition of **3** under RAPET conditions at 700 ^{o}C; lines are indexed to tetragonal MgWO$_4$ (PDF 52-0390; line marked $\bullet$ are present in the PDF file but are unindexed.

Figure 6.   Electron micrograph images of the products of the thermal decomposition of **1** under RAPET conditions at 700 ^{o}C : (a, b) TEM, bar = 50 nm, (c) SEM, bar = 100 nm.

Figure 7.   Electron micrograph images of the products of the thermal decomposition of **3**

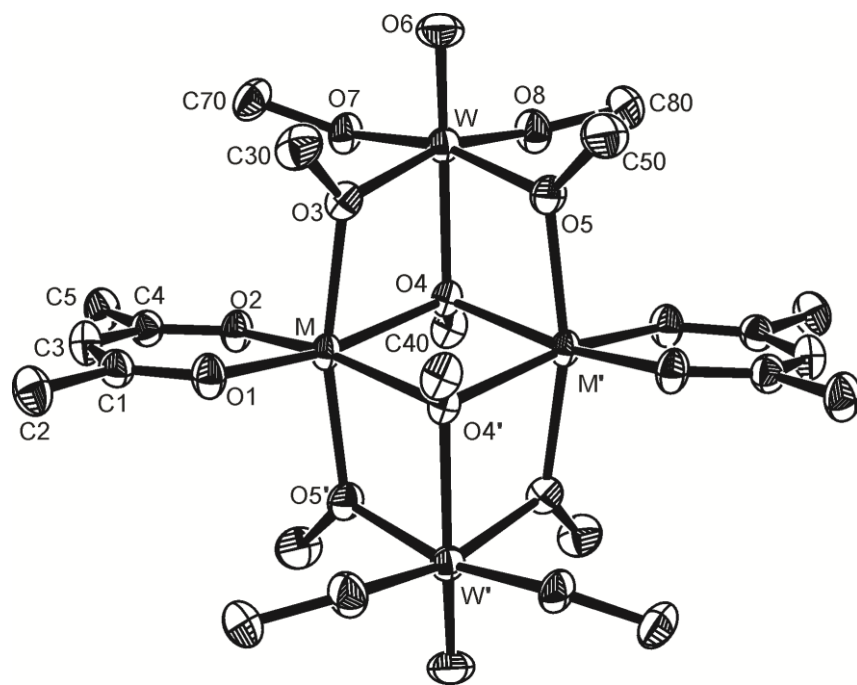under RAPET conditions at 700 ^{o}C : (a) SEM bar = 10 μm, (b) TEM bar = 50 nm.
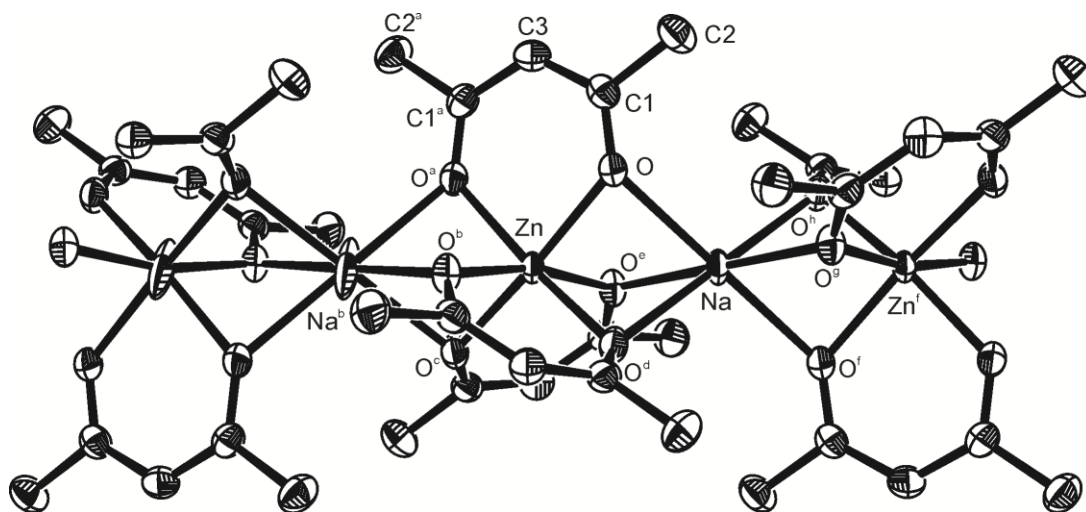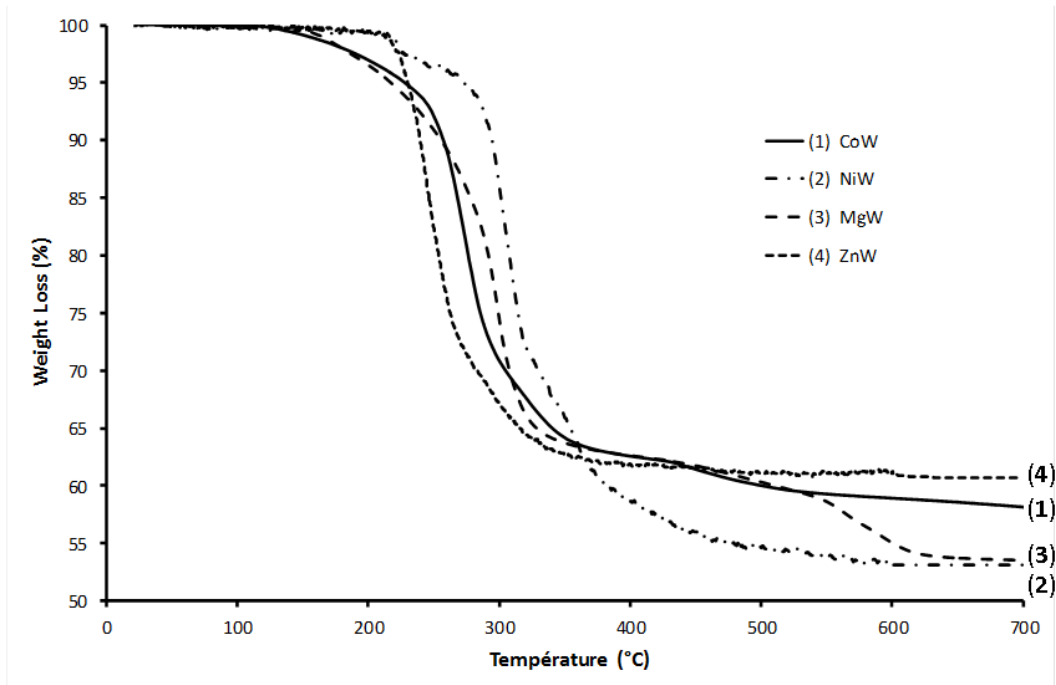
Fig. 1

Fig 2

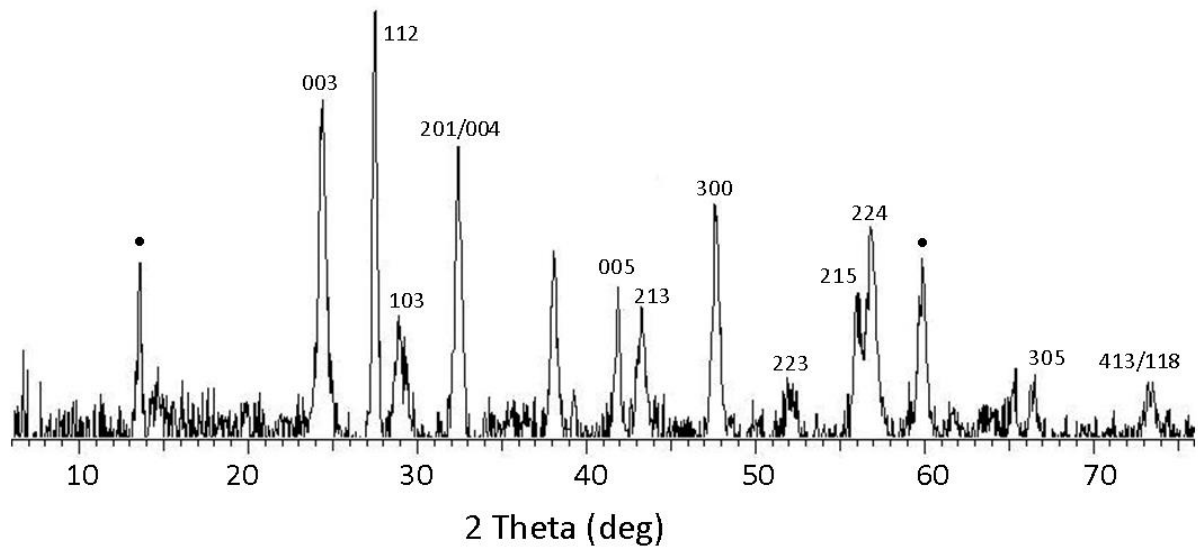**Fig 3**

Fig 4

Fig 5

(a)   (b)   (c)

Fig 6

(a)

(b)

Fig 7